Materials Today Bio 22 (2023) 100782

Contents lists available at ScienceDirect

Materials Today Bio

journal homepage: www.journals.elsevier.com/materials-today-bio

Multifunctional polysaccharide composited microneedle for oral ulcers healing

Yiyu Zeng [a,1], Yijun Gao [a,1], Liming He [b], Wenhui Ge [a], Junhui Liu [c], Yi Yu [a], Xiaoyan Xie [a,*]

[a] Department of Stomatology, The Second Xiangya Hospital, Central South University, Changsha, 410011, PR China
[b] Department of Stomatology, Changsha Stomatological Hospital, Changsha, 410004, PR China
[c] Xiangya Stomatological Hospital & Xiangya School of Stomatology, Central South University, Changsha, 410000, PR China

ARTICLE INFO

Keywords:
Oral ulcers
Polysaccharide
Microneedle
Hyaluronic acid
Wound healing

ABSTRACT

Oral ulcers have periodicity and recurrence, and the etiology and causative mechanisms remain unclear; therefore, it is difficult to treat oral ulcers effectively. Current clinical treatment methods mainly include pain relief and administration of anti-inflammatories to prevent secondary infections and a prolonged recurrence cycle. However, these traditional treatment methods are administered independently and are susceptible to muscle movements and constant salivary secretion in the mouth, resulting in ineffective drug functioning. Therefore, development of a novel treatment to reduce wound infection and accelerate wound healing for oral ulcers is required for effective treatment. Herein, we report a multifunctional polysaccharide composite microneedle patch based on hyaluronic acid (HA) and hydroxypropyl trimethyl ammonium chloride chitosan (HACC) loaded with dexamethasone (DXMS) and basic fibroblast growth factor (bFGF) for oral ulcer healing. DXMS and bFGF encapsulated the HA tip portion of the microneedle patch, endowing the microneedle patches with anti-inflammatory and angiogenic properties. HACC was applied to the back of the microneedle patch, adding antibacterial properties. The experimental results indicated that the prepared dressings exhibited good antibacterial activity and effectively promoted cell migration growth and angiogenesis. More importantly, animal experiments have shown that multifunctional microneedle patches can effectively promote oral ulcer healing. Thus, these novel multifunctional polysaccharide composite microneedle patches have great potential for oral ulcers treatment.

1. Introduction

Oral ulcer is one of the most common oral mucosal diseases , with a prevalence ranging from 5% to 20% [1–3]. Although oral ulcers have self-limiting properties and most often heal within 2 weeks, some patients experience a “continuous rise and fall” of ulcers, which persist in the oral cavity for an extended period and seriously impacts physical and mental health [4]. At present, the etiology and causative mechanisms of oral ulcers remain unclear [5]. Therefore, clinical treatment mainly focuses on treating symptoms, such as by reducing inflammation and pain, to prevent infection and promote healing [6]. Because of significant individual differences in the cause and degree of disease among patients, there is a need for a more effective treatment method. Currently, local treatment remains the first choice of treatment for oral ulcers. Commonly used drugs include glucocorticoids, healing-promoting drugs, mucosal protective agents, and antibacterial drugs [7]. Most local drugs for oral ulcers are used alone in the form of gargles, gels, buccal tablets, films, and sprays, and have a single effect. In addition, local drug use is affected by muscle movement and continuous secretion of saliva in the mouth, which shortens the action time of the drug in the mouth, leading to a decrease in the effective drug concentration at the lesion, thus significantly weakening its therapeutic effect [8]. Therefore, it is necessary to develop a new method that can simultaneously reduce infection and accelerate wound healing without affecting muscle movement, which is particularly important for the treatment of oral ulcers.

Microbial communities colonizing the oral mucosa can influence the progression of oral ulcers [9]. Disorders of the immune system also play a crucial role in the development of oral ulcers [10]. Decreased levels of growth factors in the wound environment usually lead to ischemia at the

* Corresponding author.
E-mail address: xyxie@csu.edu.cn (X. Xie).
[1] These authors contributed to the work equally..

https://doi.org/10.1016/j.mtbio.2023.100782
Received 21 May 2023; Received in revised form 24 August 2023; Accepted 28 August 2023
Available online 29 August 2023

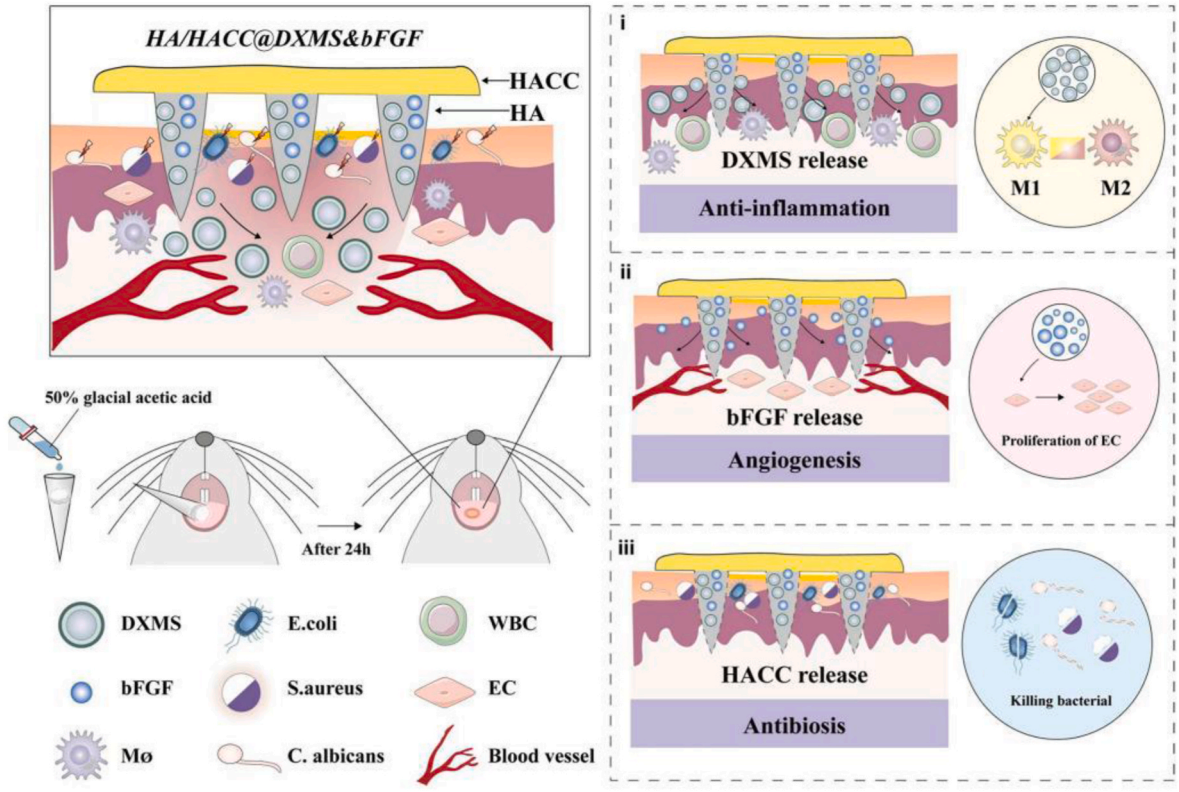

Fig. 1. Schematic presentation of the application of multifunctional HA/HACC composited microneedles patches for promoting oral ulcers healing. HACC, hydroxypropyl trimethyl ammonium chloride chitosan; HA, hyaluronic acid; DXMS, dexamethasone; bFGF, basic fibroblast growth factor; E. coli, *Escherichia coli*; S. aureus, *Staphylococcus aureus*; C. albicans, *Candida albicans*; WBC, white blood cell; EC, endothelial cell.

lesion site and impaired tissue regeneration, which affects ulcer healing. The pseudomembrane on the ulcer surface leads to the failure of the commonly used clinical drug delivery route to effectively penetrate the mucosa and exert its effects. Interactions between various factors can further the extent of oral ulcers. Microneedle (MN) patches can simultaneously load multiple drugs and penetrate the epidermis to form micropores [11]. The patches combine the advantages of a subcutaneous injection needle and transdermal patch so that drugs can directly penetrate the dermis, promote drug penetration in a minimally invasive and painless manner [12], and promote intradermal and transdermal delivery of vaccines or peptides [13,14]. Using MN patches to carry various drugs to treat oral ulcers can solve existing problems related to short local drug action time, low effective concentration, and single efficacy. Hence, the application of MN patches for oral ulcers is an effective treatment option.

Inspired by the pathogenesis of oral ulcers, we developed multifunctional polysaccharide composite MN patches for oral ulcer healing. Dexamethasone (DXMS) is a long-acting glucocorticoid that reduces inflammation by inhibiting the migration of polymorphonuclear leukocytes and reducing capillary permeability, and can therefore be used in the treatment of oral ulcers [15,16]. The basic fibroblast growth factor (bFGF) is a polypeptide that exhibits potent angiogenesis and can stimulate cell proliferation and migration [17–19]. Hydroxypropyl trimethyl ammonium chloride chitosan (HACC) and hyaluronic acid (HA) are two common polysaccharides that are widely used in the repair of skin wounds because of their biocompatibility, rapid response, and good degradability, as well as their rich, hydrophilic, living-tissue-like softness and elasticity of the stimulus response pattern [20–22]. Recently, chitosan and its derivatives have become effective ways to deliver oral drugs [23]. HACC is a water-soluble chitosan derivative with better antibacterial activity than chitosan [24], so it has better application prospects as a wound dressing. HA is a biopolymer with biological activity and is widely present in the human body. It can increase the stability of drug delivery [25], improve drug permeability, and promote wound healing in the oral cavity [26]. HA has excellent mucosal adhesion [27], allowing it to act as a barrier in the protective hydration layer formed on the ulcer wound surface, protect the wound surface, and isolate external stimuli from the nerve endings in the mucosal tissue to relieve pain and shorten the ulcer healing time [28]. Thus, the development of a HACC/HA-based multifunctional drug delivery system for oral ulcer treatment is still anticipated. Herein, we report a multifunctional polysaccharide composite MN patch with antibacterial, anti-inflammatory, and angiogenic abilities for oral ulcer healing (Fig. 1).

2. Material and methods

2.1. Chemicals and drugs

HA and HACC were purchased from Bloomage Biotech (Jinan, China). DXMS (5 mg/mL) was purchased from the Xiangya Second Hospital, Central South University (Hunan, China). bFGF was purchased from GenScript ProBio (Piscataway, NJ), and lipopolysaccharide (LPS) was purchased from Biosharp. The Live & Dead Viability/Cytotoxicity Assay Kit was purchased from the Keygen Biotech Company (Jiangsu, China), and the Cell Counting Kit (CCK)-8 Cell Proliferation and Cytotoxicity Assay Kit was purchased from Biosharp (Tallinn, Harjumaa, Estonia). The Live & Dead Bacterial Staining Kit was purchased from Yeasen (Shanghai, China). All solvents and reagents used in this study were of analytical grade.

2.2. Cell culture

Human oral fibroblasts (HOrF) and human umbilical vein

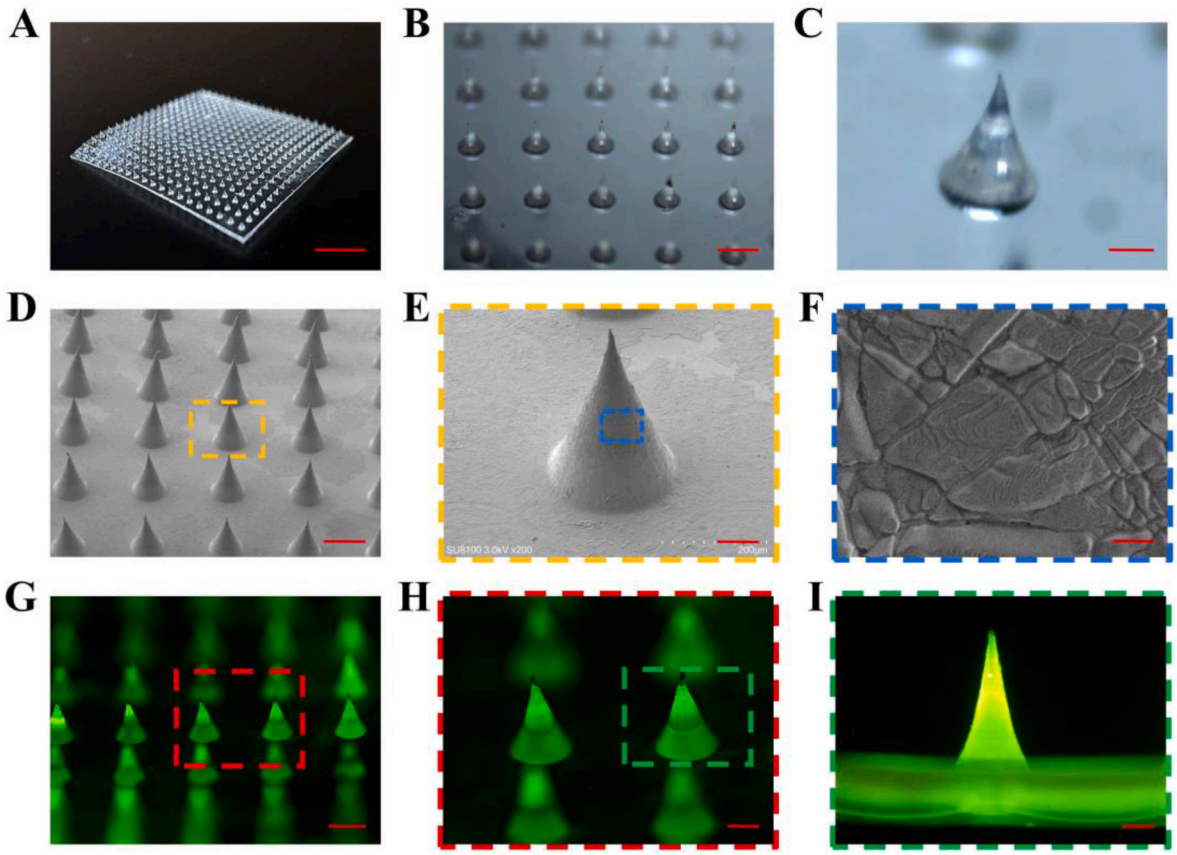

Fig. 2. Characterization of HA/HACC MN patches. (A–C) Images of intact and magnified MN patches based on optical microscopy. (D–F) SEM images showing surface microstructures. (G–I) Fluorescence images of the tip of the HA/HACC MN patches loaded with Lumisphere. Scale bars respectively are (A) 5 mm, (B, D, G) 500 μm, (C, E, H) 200 μm, (F) 10 μm and (I) 100 μm.

endothelial cells (HUVEC) were provided by the second Xiangya Central Laboratory (Changsha, China). Mouse macrophages (RAW264.7) cell lines were purchased from Abiowell (Changsha, China) and cultured in a high-glucose medium (DMEM) containing 10% FBS. All cells were maintained at 37 °C in an incubator with 5% CO_2.

2.3. MN patch preparation and characterization

We purchased a polymethylsiloxane (PDMS) mould from Shiling Laker Mould Merchant (Guangzhou, China). HA powder was dissolved in phosphate-buffered saline (PBS) to obtain a 10% (w/v) HA solution, and the HACC solid was dissolved in PBS to obtain a HACC solution. DXMS and bFGF were added, mixed with the HA solution and centrifuge at 12,000 rpm for 30 min. The mixed solution was then spread into the PDMS mould, and a lyophiliser was used to remove bubbles under negative pressure for 30 min. Next, the following steps were performed: Remove the excess HA solution containing different components on the back of the MN patch, retain the HA solution on the tip, and add the HACC solution to form the back of the MN patch. Heat and dry for 2–3 h in a drying oven at 30–35 °C to remove excess moisture. Finally, the PDMS mould was peeled off to obtain HA/HACC with different components and stored at 4 °C for future use. The morphological features of the MN patch were characterised using a stereomicroscope (JSZ6S, Jiangnan Novel Optics, Jiangsu, China) and scanning electron microscopy (SEM). To visualise the structure of the MN patches, fluorescent probe-loaded MN patches were prepared and imaged using confocal laser scanning microscopy (CLSM, Zeiss LSM 710, Jena, Germany). Lumisphere was used as a fluorescent probe to show the tip morphology.

2.4. Physical properties of MN patch

I) Mechanical Test

To ensure that the HAMN has sufficient strength to penetrate the oral mucosa without fracture, we applied a force gauge (Handpi NK-50, Shenzhen, China) to test the mechanical properties of the MN patch. The MNs were attached to a horizontal platform with the needle tip facing upward. The probe was moved downward perpendicular to the MNs at a constant speed of 0.1 mm/min. The maximum support force (N/microneedle) of each tip can be calculated from the value of the force divided by the number of tips.

II) In vivo mucosa penetration ability

The Rhodamine B (RhoB)-loaded HA/HACC MN patch was inserted into the normal buccal mucosa of Sprague–Dawley rats. Frozen sections of rat mucosa were then prepared. The depth of MN patch penetration into the oral mucosa was observed using a fluorescence microscope. Changes in the oral mucosal epithelium after treatment with MN patches were also observed using hematoxylin and eosin (H&E) staining. Insertion depth was measured using ImageJ software.

III) Dissolution properties

The dissolution properties of microneedles were tested using rat oral mucosa. The HA/HACC@DXMS&bFGF were pressed into the lower lip mucosa of rats and continued for 30s, 1 min and 2 min respectively, and the MN patches were removed at different time points to observe the dissolution under light microscopy.

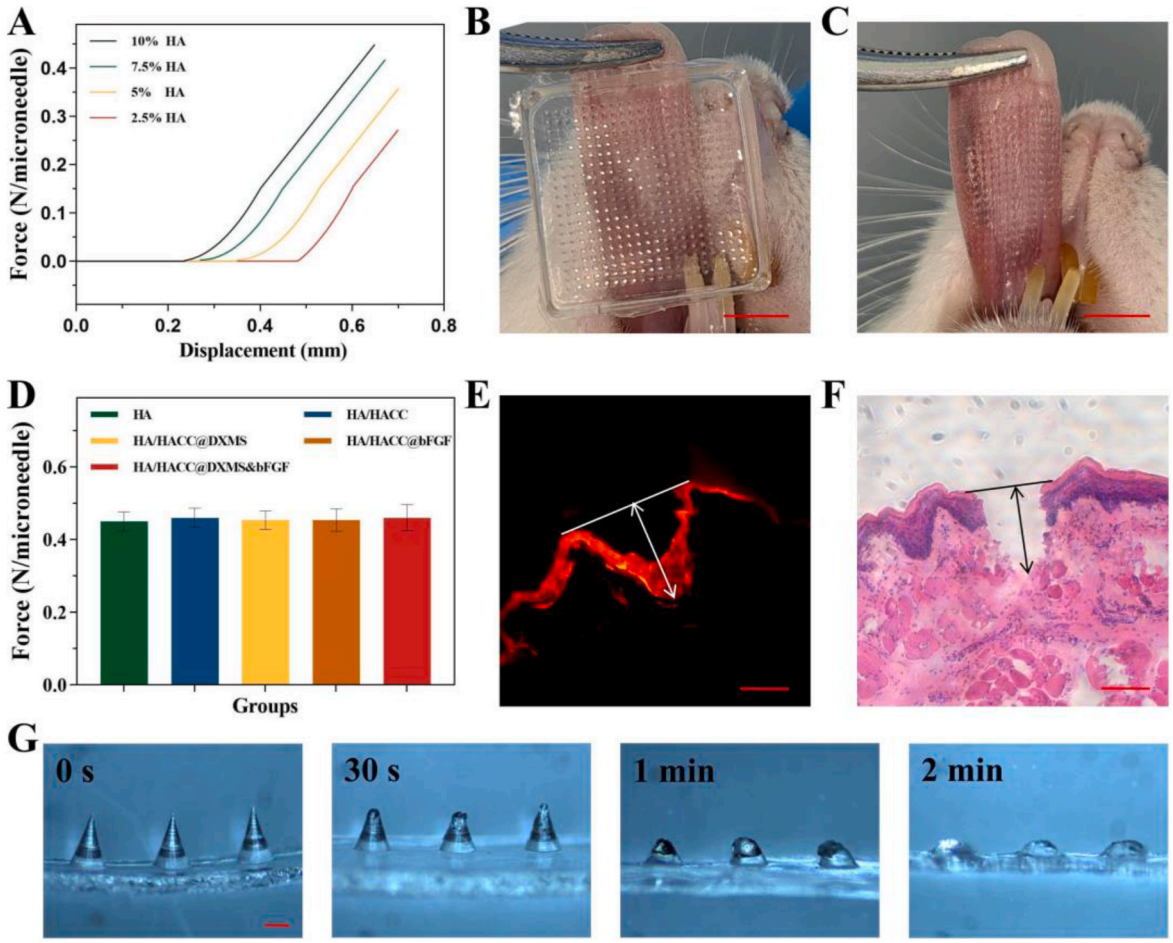

Fig. 3. Physical properties of MN patches. (A) Mechanical strength of the MN patch with different concentrations of HA. (B, C) The penetration assay in rat oral mucosa. (D) Mechanical strength of different MN patches. (E) The red fluorescent RhoB-loaded MN patches is tightly attached to the mucosal surface. (F) HE staining images after MN patch puncture. (G) The MN patch can be completely dissolved within 2 min. The scar bar are (B, C) 5 mm and (E, F, G) 200 μm. (For interpretation of the references to color in this figure legend, the reader is referred to the Web version of this article.)

2.5. *In vitro and in vivo biocompatibility assays*

I) Calcein-AM/propidium iodide (PI) staining: HA, HA/HACC, HA/HACC@DXMS, HA/HACC@bFGF, and HA/HACC@DXMS&bFGF were dissolved in 1 mL of culture medium containing 10% FBS and filtered to obtain a sterile filtrate for use. HOrF and HUVEC were inoculated separately in 96-well plates and incubated for 24 h. This step was followed by intervention using sterile filtrate from each group of MN patches for 24 h. After treatment, the cells were fluorescently labelled with calcein-AM/PI staining. Finally, the results were examined by fluorescence microscopy. The corresponding culture medium of various cells was used as a negative control. Live cell (%) = live cell (green)/[live cell (green) + dead cell (red)] × 100% (the percentage of viable cells in the control group was set at 100%).

II) Hemolysis test: Fresh rat blood (1 mL) was stirred with a glass rod to extract the fibrinogen. After removing the fibrotic blood, the supernatant was aspirated after centrifugation at 2000 rpm for 5 min. Then, the red blood cells were washed with 10 mL PBS three times, the supernatant was removed, and the red blood cell precipitate was obtained. Red blood cells (100 μL) were added to 5 mL of PBS to prepare a 2% red blood cell suspension, and MN patches were added to each group, respectively. After 2 h, the erythrocyte suspension was centrifuged at 2000 rpm for 5 min, the supernatant was added to a 96-well plate, and the optical density (OD) at 529 nm was measured using an ultraviolet–visible spectrophotometer. Triton X-100 (1% v/v) was used as a positive control (100% reference value for hemolysis). Hemolysis (%) = [OD(treatment group) - OD(PBS)]/[OD(Triton X-100) - OD (PBS)] × 100%

III) *In vivo* drug toxicity: HE staining of vital organs (the heart, liver, spleen, lungs, and kidneys) was performed to observe drug toxicity *in vivo*.

2.6. *CCK8 assay*

HOrF and HUVEC were grown in 96 well plates with a seeding density of 4×10^3. Cells in the exponential growth phase were treated with different groups (control, HA, HA/HACC, HA/HACC@DXMS, HA/HACC@bFGF, and HA/HACC@DXMS&bFGF) and incubated for 24 h. Subsequently, the cells were incubated with CCK8 kit for 2 h. Cell viability was demonstrated by measuring the OD at 450 nm. Cell viability (%) = [OD(treatment group) - OD(blank group)]/[OD (control group) - OD(blank group)] × 100%.

2.7. *Wound healing assay*

MN patches were dissolved in 1 mL of cell culture medium without FBS and filtered to obtain a sterile filtrate for use. HOrF and HUVEC were inoculated in 6-well plates and cultured in cell culture medium containing 10% FBS, and when their growth was confluent to 80%, they were scored using a 200 μL pipette tip. Interventions were performed

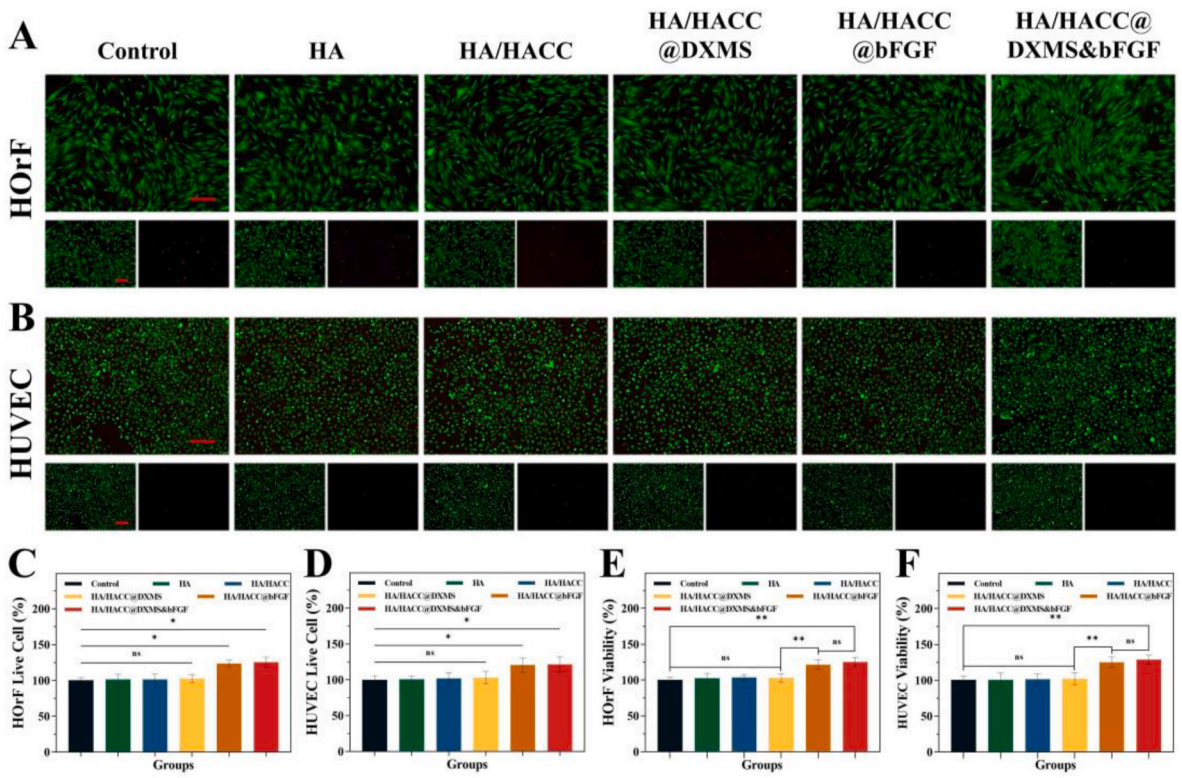

Fig. 4. Investigation of biocompatibility ability and cell viability of MN patches. (A) Live/dead fluorescent images of HOrF. (B) Live/dead fluorescent images of HUVEC. (C) Quantitative Statistics of HOrF live cells. (D) Quantitative Statistics of HUVEC live cells. (E) CCK8 cell viability assay of HOrF. (F) CCK8 cell viability assay of HUVEC. The scale bars are 100 μm *p < 0.05, **p < 0.01, ***p < 0.001, ****p < 0.0001.

using cell culture medium without FBS and a sterile filtrate from each MN patch group. Images were observed using light microscopy at 0 and 24 h after the intervention, and the wound size was quantified using ImageJ software. The migration rate (%) = (scratch distance - distance after growing)/scratch distance × 100%.

2.8. Tube formation assay

Extracellular matrix gel was mixed with DMEM at a 1:1 ratio on ice, and 50 μL was added to a 96-well plate and incubated for 1 h at 37 °C in a cell culture incubator. Cells were pendant suspended from the control, HA, HA/HACC, HA/HACC@DXMS, HA/HACC@bFGF, and HA/HACC@DXMS&bFGF solutions. The cell concentration was adjusted to 1×10^5 cells/mL. In total, 100 μL of cell suspension was added uniformly to the prepared gels and incubated in the medium for 6 h before capturing images of tubule formation by microscopy after fluorescent staining. Quantitative statistical analysis was performed using ImageJ software.

2.9. In vitro and in vivo antimicrobial assays

Escherichia coli, *Staphylococcus aureus*, *Streptococcus mutans* and *Candida albicans* were used to assess the antibacterial capacity of the HACC backing plates. *E. coli*, *S. aureus*, and *C. albicans* are cultured on ordinary agar plate, and *S. mutans* is cultured on blood agar plate.

I) Inhibition loop method: A 10^6 CFU/mL bacterial suspension was inoculated into a solid agarose Petri dish and spread evenly with a smear stick. Six-mm round filter paper was immersed into the sterile filtrate from each MN patch group for 5 min, then placed on a plate with a bacterial medium, and incubated for 24 h (37 °C) to observe the presence or absence and size of the inhibition ring around the round piece of filter paper.

II) Coating of plates: A bacterial suspension (10^6 CFU/mL) was mixed with the sterile filtrate from each MN patch group and incubated at 37 °C for 24 h. After incubation, the bacterial suspension was diluted 1000 times, inoculated onto the surface of a solid agarose Petri dish, and incubated at 37 °C for 24 h. The Petri dish was removed and photographed to count and calculate the inhibition rate.

III) Live dead staining: A bacterial suspension (10^6 CFU/mL) was mixed with the sterile filtrate from each MN patch group, and incubated at 37 °C for 24 h. At the end of incubation, the bacterial suspension was stained according to the Live & Dead Bacterial Staining Kit manufacturer's method.

2.10. In vitro assessment of anti-inflammatory potential

RAW264.7 macrophages were inoculated into 96-well plates. Cells were pretreated with 200 ng/mL of LPS for 24 h to construct an inflammatory model. Cells were treated with HA/HACC@DXMS&bFGF sterile filtrate. After 24 h, the supernatant was collected from the 96-well plates, and the inflammatory factors levels in the culture medium were measured using enzyme-linked immunosorbent assay kits for tumour necrosis factor (TNF)-α and interleukin (IL)-6 (Multisciences, Hangzhou, China).

2.11. Construction of an animal model for oral ulcers in vivo

All animal studies were ethically supported and approved by the Ethics Committee of the Xiangya Second Hospital, Central South University and all animal experiments were carried out in accordance with the Care and Use of Laboratory Animals. Thirty-six male rats were anaesthetised with isoflurane gas and burned with 50% glacial acetic acid to establish an oral ulcer model with a diameter of 5 mm. 24 h later, the experimental area showed obvious ulcers with a yellowish-white

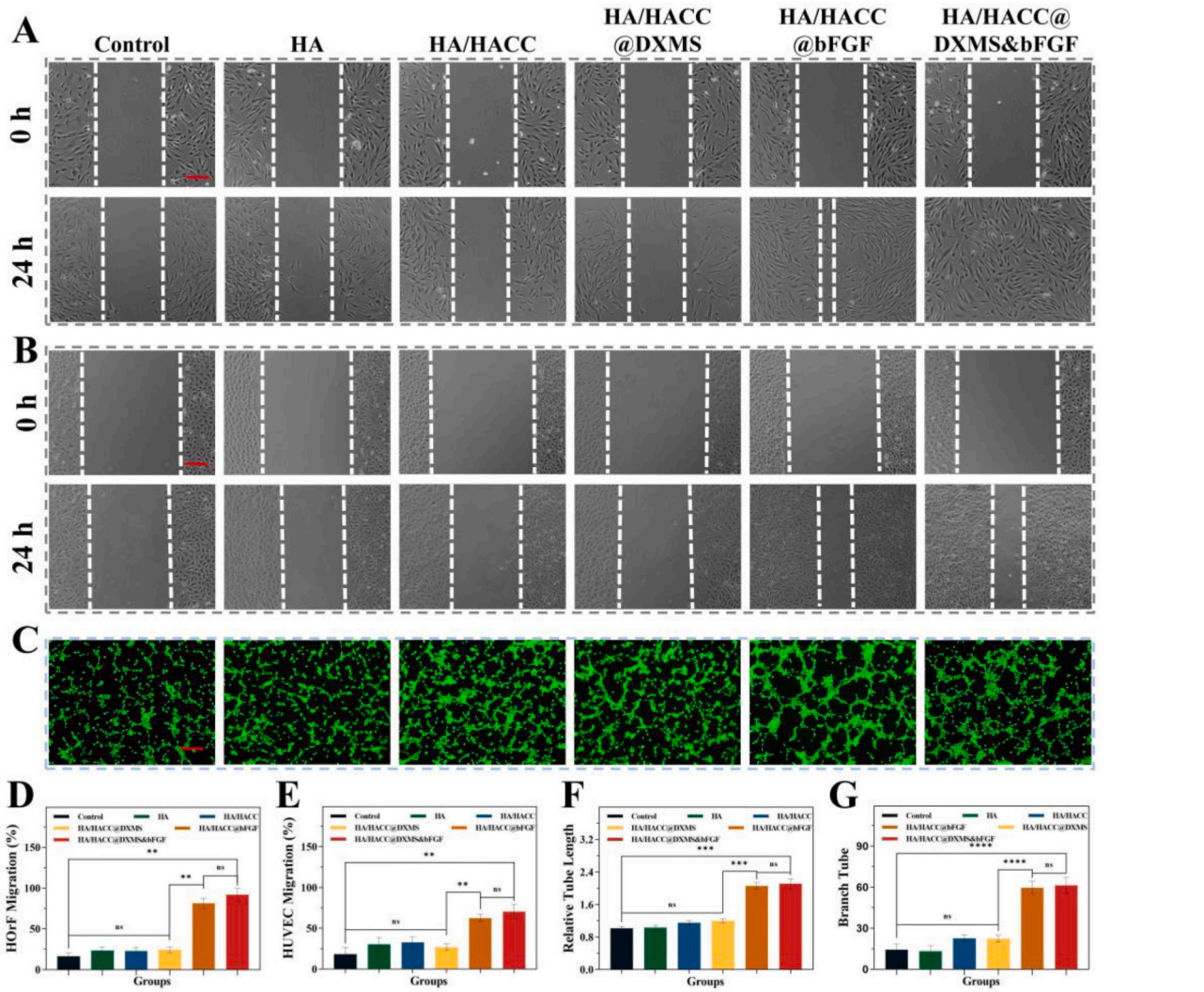

Fig. 5. Evaluation of migration and angiogenesis ability *in vitro*. (A) Representative images of the cell migration assay of HOrF after different treatments. (B) Representative images of the cell migration assay of HUVEC after different treatments. (C) Fluorescence images of calcein-AM labeling HUVEC tube formation after various treatments. (D) Quantitative analysis of cell migration of HOrF. (E) Quantitative analysis of cell migration of HUVEC. (F) Analysis of tube length results. (G) Analysis of branching tubes. Scale bars are 100 μm *p < 0.05, **p < 0.01, ***p < 0.001, ****p < 0.0001.

surface and some ulceration and oozing, indicating successful modelling. After successful modelling, the rats were randomly divided into six groups: control, HA, HA/HACC, HA/HACC@DXMS, HA/HACC@bFGF, HA/HACC@DXMS&bFGF.

MN patches were cut to the appropriate size (completely covering the ulcer wound) for use. They were applied to the affected part of the rats' oral ulcers during administration and gently pressed for 20 s to ensure that the MN patches fit closely to the affected part. The drug was administered once daily for 5 consecutive days after the model was successfully established. The control group was left untreated. Changes in the area of oral ulcers were recorded and photographed daily. The wound area and oral ulcer healing rate were measured using ImageJ software on Day 1–6. On the 6th day of treatment, HE and Masson stainings were performed to assess healing and collagen deposition in the lesion areas.

2.12. Immunohistochemical analysis

Immunohistochemical (IHC) staining of TNF-α and IL-6 was conducted to detect tissue inflammation; IHC staining of CD31 and α-smooth muscle actin (α-SMA) was performed to observe angiogenesis; and IHC staining of F4/80, CD86 and CD206 was performed to detect macrophage polarization.

2.13. Statistical analysis

All experimental data were analysed using GraphPad Prism (GraphPad Software, La Jolla, CA). Statistical differences between the data were assessed using one-way analysis of variance, and all data are presented as mean ± standard deviation. Statistical significance was set at $p < 0.05$.

3. Results and discussion

3.1. Characteristics of HA/HACC MN patches

The fabricated multifunctional MN patch was observed using light microscopy, SEM and CLSM. The MN patch consisted of an array of 400 (20 × 20) complete and continuous needles (Fig. 2A–C), each presenting a triangular pyramidal shape with a height of 430 μm and spacing of 700 μm (Fig. 2D–F). The surfaces of the back and tip of the MN were smooth, indicating that HA/HACC was successfully manufactured. This structure was able to effectively penetrate the mucosa. A needle tip layer loading of the lumisphere was observed with CLSM, indicating that the

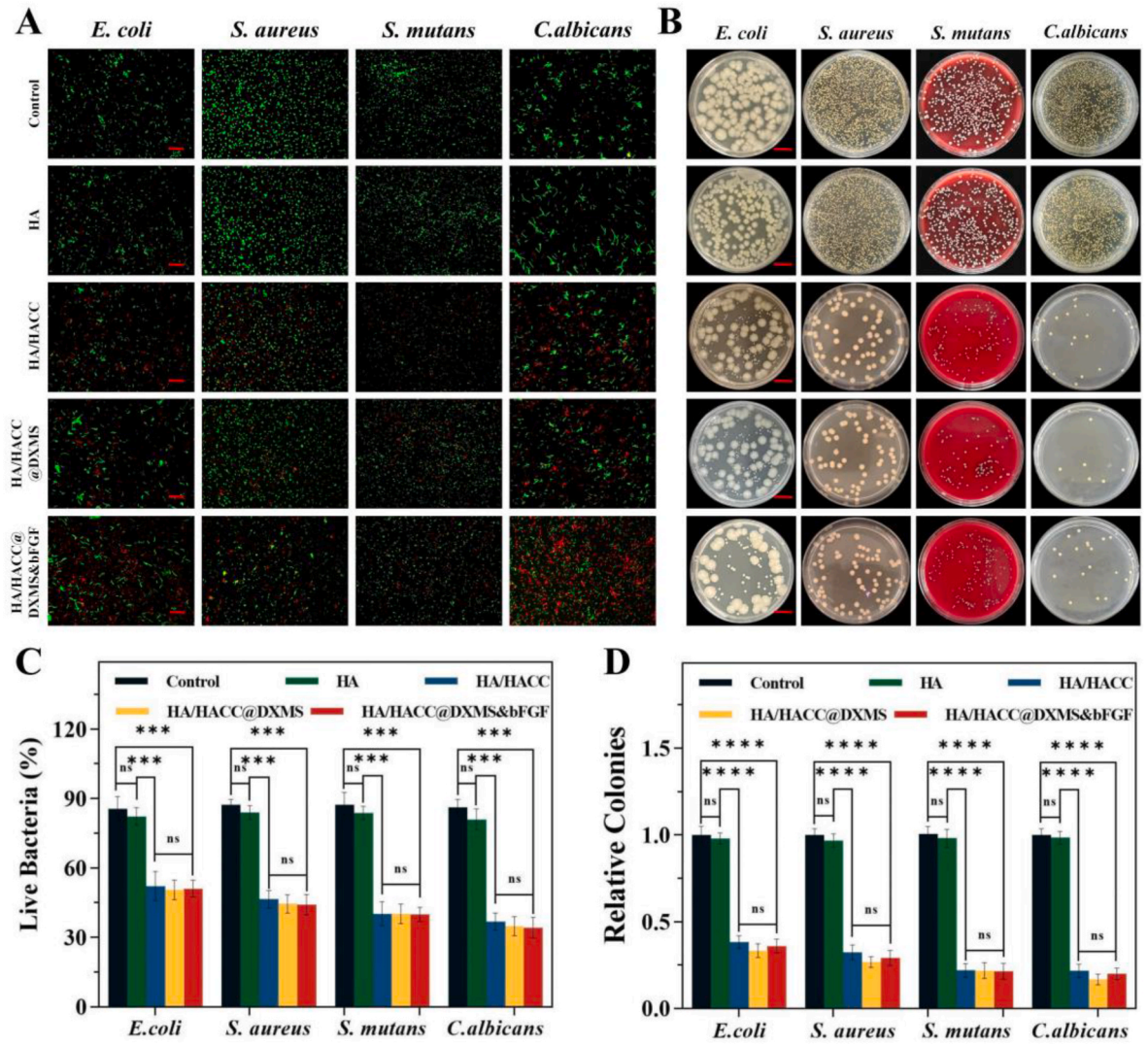

Fig. 6. Investigation of the antibacterial ability of MN patch. (A, C) Fluorescence imaging and live bacteria rate of *E. coli*, *S. aureus, S. mutans* and *C. albicans*. (B, D) Plate coating results and colony counting of *E. coli*, *S. aureus, S. mutans* and *C. albicans*. The scale are (A) 100 μm and (B) 1 cm *p < 0.05, **p < 0.01, ***p < 0.001, ****p < 0.0001.

needle tip HA and dorsal HACC could form a single unit (Fig. 2G–I).

3.2. Physical properties of MN patches

The maximum support force (N/microneedle) of each tip of different MN patches was tested to ensure that the MN patches had sufficient strength to penetrate the oral mucosa without breaking. As shown in Fig. 3A, 10% HA had better mechanical properties and could withstand greater force without displacement. There was no statistical difference in the maximum support force of HA/HACC, HA/HACC@DXMS, HA/HACC@bFGF, HA/HACC@DXMS&bFGF compared to that of 10% HA patch alone (Fig. 3D). Also, the addition of HACC, DXMS and bFGF did not affect the mechanical strength of the microneedle patches. To study the penetration ability of MN patches, HA/HACC@DXMS&bFGF were applied to rat oral mucosa for observing the array of MN patches. The corresponding insertion points could be observed after the removal of HA/HACC@DXMS&bFGF (Fig. 3B and C). In addition, the distribution of DXMS using fluorescent labelling can be observed at the tip site. The results showed that the needle tip of the MN patch successfully penetrated the epidermis, where penetration depth reaches 400 ± 8 μm, and dissolved almost completely in the oral mucosa (Fig. 3E). H&E staining showed that a microporosity generated by MN patches was found in the oral mucosal tissue at a depth of 380 ± 5 μm (Fig. 3F). Due to the elasticity of the oral mucosa, the depth of the microporosity was less than the height of the MNs [29]. However, it was clearly observed that the MNs had penetrated the epithelial and lamina propria to reach the submucosa. The loaded drug is released and diffused as the microneedle dissolves. As shown in Fig. 3F, the MN patches dissolved almost completely within 2 min. Therefore, in the subsequent animal experiments, we took a 2-min treatment time to ensure the release of the loaded drug. Overall, the findings suggest that HA/HACC@DXMS&bFGF have sufficient strength to penetrate the oral mucosa without fracture and can directly target the loaded drug to the deep part of ulcers, and have a rapid drug release capacity.

3.3. Biocompatibility and cell viability of HA/HACC patches in vitro

Good biocompatibility is a prerequisite for the application of various material components in the biomedical field [30]. We chose HOrF and HUVEC for exploring the effects of microneedle patches on oral mucosal cells. After staining the cells with calcein-AM/PI, after 24 h of incubation, the morphology of the cells in each group was normal and healthy. The proportion of live cells in all groups was greater than that of the control group (Fig. 4A–D). Fig. 4E and F shows the cell viability of HOrF

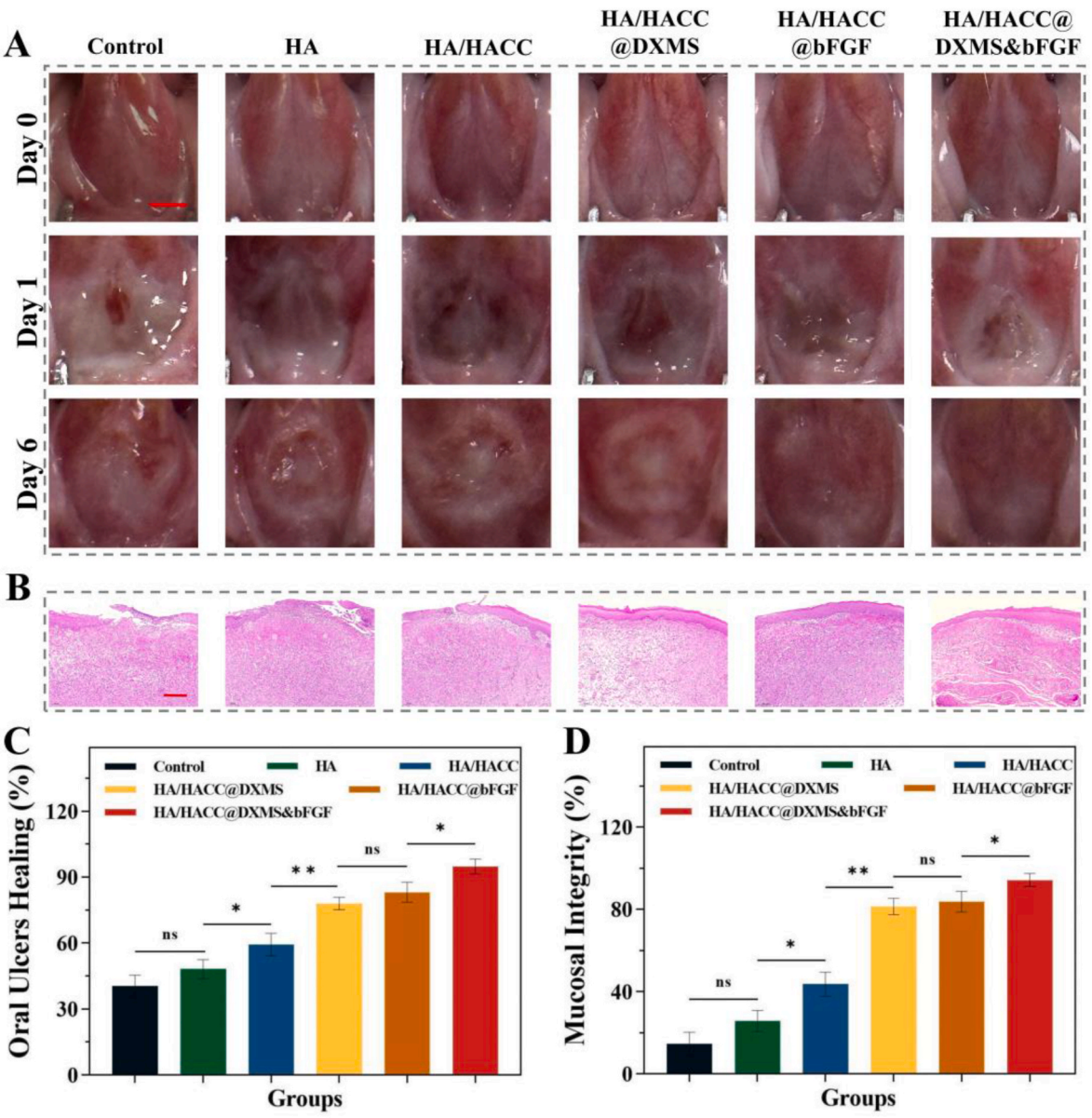

Fig. 7. Healing of oral ulcers in rats after treatment. (A) Image of rats oral ulcers on Day 0, Day 1 and Day 6 of treatment. (B) HE staining images of oral ulcers tissue on Day 6. (C) Percentage of oral ulcer repaired on Day 6. (D) Oral mucosal epithelial integrity in rats on Day 6 of treatment. Scale bars are (A) 250 μm, and (B) 100 μm respectively. *p < 0.05, **p < 0.01, ***p < 0.001, ****p < 0.0001.

and HUVEC after different MN patch treatments. The CCK8 experiment results showed that, compared with the control group, MN patches containing bFGF significantly increased the viability in both two cell types. The above results showed that our MN patch has excellent biosafety and significantly promotes cell activity and proliferation with broad application prospects in the treatment of oral ulcers.

3.4. Cell migration and angiogenesis of HA/HACC MN patches in vitro

To shorten the duration of oral ulcers, we added pro-healing ingredients to the MN patch to accelerate cell proliferation. We assessed the effects of HA containing different concentrations of bFGF on the migration and proliferation of HUVEC and HOrF. When its concentration reached 1 μg/mL, HUVEC and HOrF showed the fastest migration to the scratch centre and the highest cell proliferation (Fig. S1). Therefore, we used 1 μg/mL bFGF in the follow-up experiment. The results of the scratch healing migration assay showed that after 24 h of treatment, HOrF treated with HA/HACC@bFGF and HA/HACC@DXMS&bFGF had a significantly increased migration rate (Fig. 5A, D), while HACC and DXMS did not affect cell migration in the wound healing assay. We also observed consistent results in HUVEC (Fig. 5B, E). During the cell proliferation and granulation phase, bFGF promotes the formation of new capillaries, which significantly increases the number of capillaries and blood flow in the granulation tissue, improves microcirculation, and provides oxygen and nutrients necessary for tissue repair [31]. The angiogenic potential of MN patch was determined by *in vitro* tube formation assay. Treatment HA/HACC@DXMS&bFGF resulted in a significant increase in the total tube length and the number of branching tubes of HUVEC, indicating that HUVEC can respond to locally high bFGF expression and thus have the potential to promote neovascularization (Fig. 5C, F, G).

3.5. Anti-inflammatory of HA/HACC MN patches in vitro

Oral ulcers are a type of inflammatory disease, and their progression is mediated by various inflammatory factors, such as TNF-α and IL-6

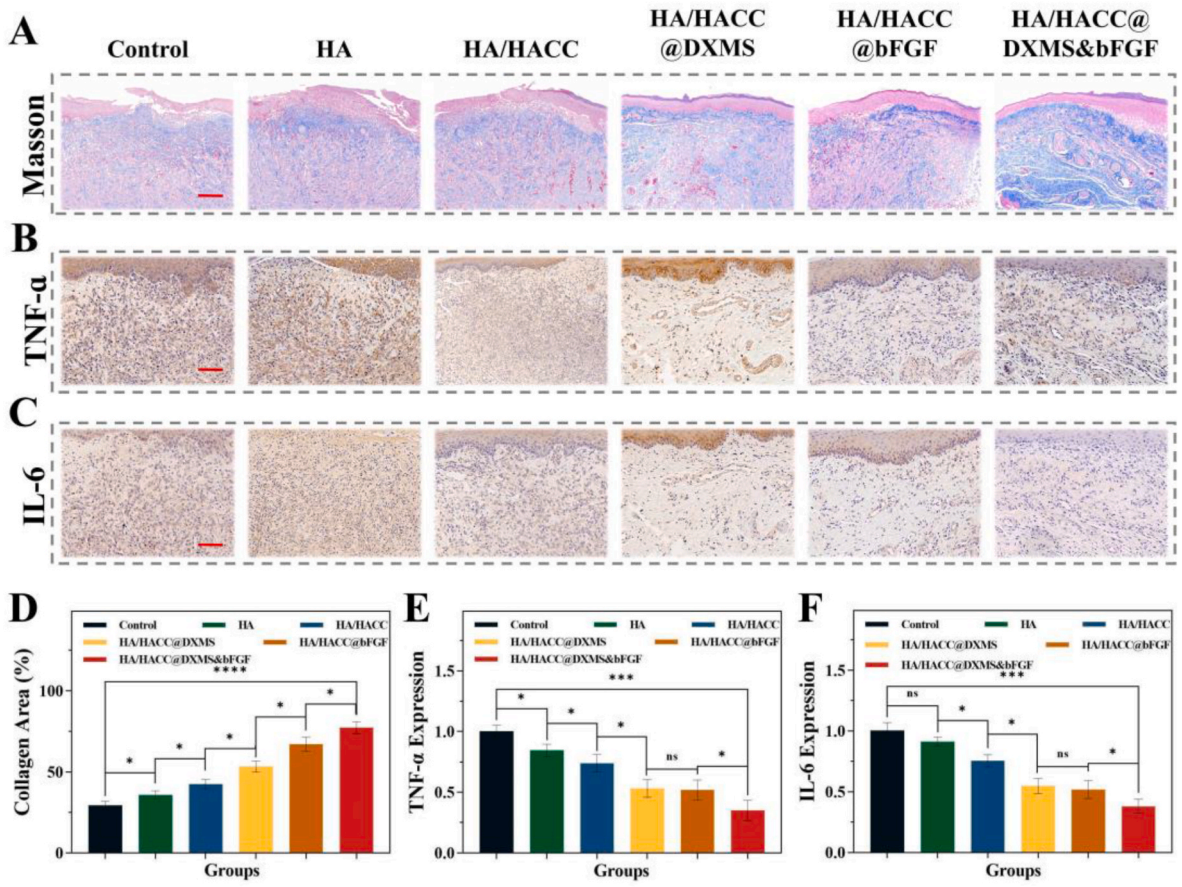

Fig. 8. Characterization of collagen deposition and proinflammatory factors. (A–C) Staining of collagen, TNF-α and IL-6. (D–F) Quantitative analysis of collagen deposition, TNF-α and IL-6 in different groups after treatment. The scale bars are (A) 100 μm and (B, C) 250 μm *p < 0.05, **p < 0.01, ***p < 0.001, ****p < 0.0001.

[32]. These inflammatory factors can induce nearby fibroblasts to release chemokines, further recruiting lymphocytes to the lesion site, ultimately leading to mucosal epithelial detachment and ulcer formation. The levels of TNF-α and IL-6 were measured in the supernatant of macrophage after LPS induction. DXMS substantially reduced the LPS-induced expression levels of TNF-α and IL-6 compared to the control group. At the same time, HA/HACC@DXMS&bFGF had consistent anti-inflammatory effects with DXMS solution, suggesting that HA does not interfere with the action of DXMS. Therefore, the multifunctional MN patch loaded with DXMS exerted an effective anti-inflammatory effect (Fig. S2).

3.6. Antibacterial ability of HA/HACC in vivo and in vitro

Oral ulcer sites have reduced defences against microorganisms, and microbial colonization of the wound site can cause infection, thereby delaying the healing process [33]. Previous studies have reported that HACC has a wide range of antibacterial and fungal activities [34]. To improve the antibacterial performance of the MN patch and reduce the use of antibiotics, HACC was added as an MN backing in this study. Studies have shown that the development of oral ulcers is associated with the colonization of *E. coli* [35]. The presence of common antigens between streptococci hemolytic and the oral mucosal epithelium can cause the development of oral ulcers through cross-reactivity [36]. And *S. aureus* and *C. albicans* also play an important role in the development of oral ulcers. Through the inhibition loop experiment, we determined the optimal concentration of HACC for antibacterial activity (Fig. S3). And in subsequent experiments, a 4% HACC was used. Fig. 6A shows images of *E. coli*, *S. aureus*, *S. mutans* and *C. albicans* stained with the live/dead stain. The control and HA groups consisted mainly of live bacteria, with a small amount of dead bacteria. In contrast, HA/HACC and HA/HACC@DXMS&bFGF showed mainly dead bacteria, with a higher ratio of dead/live bacteria than the control group (Fig. 6C). The number of bacteria was significantly reduced after co-culture with the above bacteria using HA/HACC and HA/HACC@DXMS&bFGF. As shown in Fig. 6B, D, the highest number of bacterial colonies was observed in the control group, covering almost the entire culture plate. After HACC was added, only a few colonies were found in the Petri dish. The above results showed that the multifunctional MN patches with HACC added had a wide range of antimicrobial activities, and the addition of DXMS and bFGF did not affect the antimicrobial activity of HACC.

3.7. In vivo ulcers healing assessment of HA/HACC

Encouraged by the results of the *in vitro* experiments, a glacial acetic acid-induced rat oral ulcer model was used to assess the effects of HA, HA/HACC, HA/HACC@DXMS, HA/HACC@bFGF, HA/HACC@DXMS&bFGF on ulcer surface healing. And the healing process was recorded for 6 days. On day 0, the oral mucosa of all groups of rats exhibited a uniform, smooth pink color. On Day 1, oral ulcers of rats in each group showed a round or oval ulcer (diameter 0.5 mm) covered with a yellow pseudomembrane, central depression, clear boundary, and red, swollen mucosa. No statistically significant differences were observed between the groups. After successful modelling, the rats were then treated in groups. Over time, a gradual decrease in the wound area was observed in all groups. As shown in Fig. S4, the HA/HACC@DXMS&bFGF group had the fastest wound healing speed, and the ulcer healed completely on Day 6 of treatment. In addition, HA/HACC@DXMS&bFGF could promote wound healing more significantly

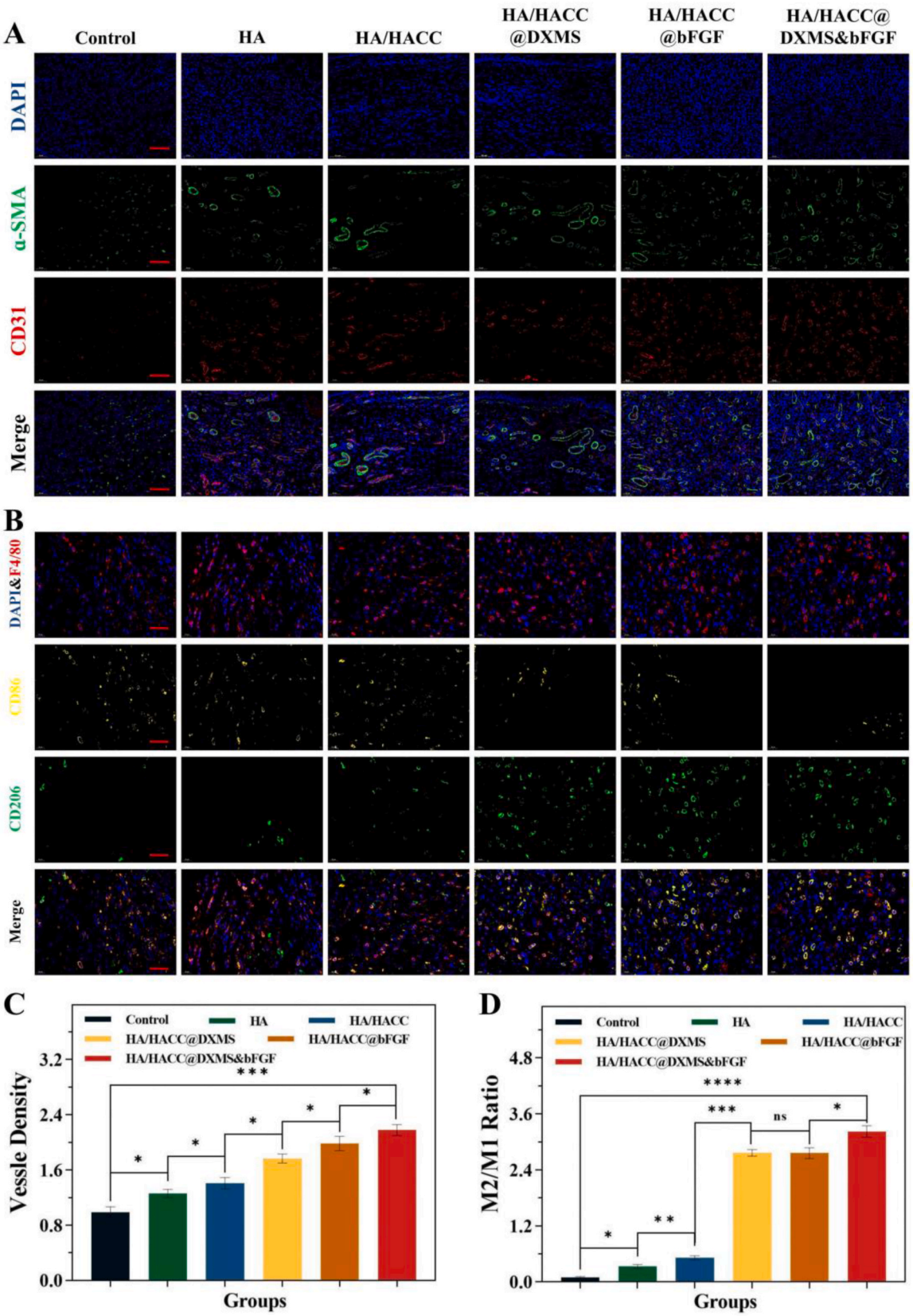

Fig. 9. Characterization of neovascularization and macrophage polarization. (A) The fluorescent images of the immunostaining of α-SMA (green) and CD31 (red). (B) The fluorescent images of the immunostaining of CD86 (yellow) and CD206 (green). (C) The analysis of vessel density. (D) The analysis of M1/M2 macrophages ratio. The scale bars are (A) 250 μm and (B) 100 μm *p < 0.05, **p < 0.01, ***p < 0.001, ****p < 0.0001. (For interpretation of the references to color in this figure legend, the reader is referred to the Web version of this article.)

compared with treatment with HA/HACC@bFGF, HA/HACC@DXMS or HA/HACC (Fig. 7A, C). The HACC back of HA/HACC@DXMS&bFGF has a favorable antibacterial effect and can provide a suitable microenvironment for the healing of oral ulcers. It can also target the delivery of DXMS and bFGF to the injury site to perform anti-inflammatory and pro-angiogenic effects. A series of synergistic effects can greatly promote the healing of oral ulcer. These results showed that HA/HACC@DXMS&bFGF significantly promoted the healing of oral ulcers in rats.

The HE staining results showed that only a small amount of epithelialized and loose disorganised connective tissue was observed in the control group (Fig. 7B). After treatment with HA/HACC@DXMS&bFGF, all layers of tissue in the ulcerated area were intact and there was no significant inflammatory response (Fig. 7D).

3.8. Histological analysis

To observe the healing of oral ulcers at a pathologic level, we further assessed collagen deposition in oral ulcer wounds using Masson staining. The control group had irregular arrangement, sparse collagen fibers, and the least collagen deposition. The healing surface of oral ulcers treated with HA/HACC@DXMS&bFGF showed denser collagen fibrils than the control group (Fig. 8A), which were arranged in parallel in the extracellular matrix more regularly. There was an increase in collagen deposition to varying degrees in all groups as compared to the control group. While collagen deposition was highest in group HA/HACC@DXMS&bFGF (Fig. 8D). We used immunohistochemical staining to assess the inflammation of the wounds. The results showed that the expression of TNF-α and IL-6 decreased in the remaining groups compared with the control group, with the greatest decrease in HA/HACC@DXMS&bFGF (Fig. 8B, C, E, F). These results suggest that HA/HACC@DXMS&bFGF has a positive anti-inflammatory effect and can effectively alleviate the inflammatory response of oral ulcers. CD31 is an endothelial marker [37], and α-SMA is abundant in smooth muscle cells of the vessel wall [38], which are commonly used as markers of neovascularization. The results of α-SMA and CD31 immunofluorescence staining showed that angiogenesis in the HA/HACC@DXMS&bFGF group was better than that in the other treatment groups (Fig. 9A, C). This is consistent with the findings of previous cell experiments. Following tissue injury, M1 macrophages secrete pro-inflammatory cytokines such as TNF-α, IL-1, IL-6, and IL-12, which have anti-proliferative functions [39]. While M2 anti-inflammatory macrophages can improve immunomodulation, tissue repair. Thus, the balanced polarization of M1/M2 macrophages determines tissue outcome in inflammation or injury. We used CD86 (yellow) and CD206 (green) immunofluorescence staining to probe the effect of microneedle patches on macrophage polarization. The results showed that both HACC, DXMS and bFGF increased the proportion of CD206-positive cells (M2 macrophages) and decreased the proportion of CD86-positive cells (M1 macrophages ()B, D)Fig. 9. The M2/M1 ratio in the tissues was the greatest on Day 6 after treatment with HA/HACC@DXMS&bFGF, suggesting the most effective repair and remodeling of the injury site. These experimental results demonstrated that we prepared HA/HACC@DXMS&bFGF with excellent tissue-repair ability (see).

A hemolysis assay was performed to assess the compatibility of the MN patch with the biological system (Fig. S5A). As shown in Fig. S5B, the control group and groups of MN patches caused hemolysis of <2% [40]. Therefore, the MN patch can be considered non-hemolytic and can be safely used as an effective drug for the treatment of oral ulcers in rats. Finally, to verify the biological safety of the prepared MN patches containing different components, we removed the critical organs of the experimental animals on Day 6 of treatment. We performed histopathological analysis of the changes in the heart, liver, spleen, lungs, and kidneys using HE staining. As shown in Fig. S5C, compared with the control group, no abnormal cells or structural changes were observed in the organs of rats treated with various MN components.

4. Conclusions

In summary, we developed a multifunctional polysaccharide composite MN patch for oral ulcers healing. This composite MN patch is independent of muscle movement and can target the therapeutic drug to the lesion in a short time compared to conventional delivery methods. In addition, it can be loaded with multiple drugs at the same time, greatly reducing patient pain by reducing infections and accelerating wound healing. These features make this composite MN patch ideal for the treatment of oral ulcers and other related diseases. HACC effectively inhibited the growth of pathogenic bacteria and created a good repair microenvironment for ulcer healing. Additionally, the dual modification with DXMS and bFGF effectively improved the anti-inflammatory properties and tissue repair ability of the MN patches, thereby accelerating ulcer wound healing. Overall, our work suggests that multifunctional HA/HACC composited MN patches containing DXMS and bFGF may be an effective treatment for oral ulcers and have other wound-healing applications.

Ethics approval

The authors declare that all animal experiments are approved by the Animal Ethical and Welfare Committee, The Second Xiangya Hospital, CSU, P.R.China (20230026) as well as the ARRIVE Guidelines. All authors comply with all relevant ethical regulations.

Funding

This study was funded by the Natural Science Foundation of Hunan Province, China (2023JJ60089).

Data statements

Data availability may be granted by contacting the corresponding author.

CRediT authorship contribution statement

Yiyu Zeng: Investigation, Writing – original draft. **Yijun Gao:** Project administration, Writing – review & editing. **Liming He:** Investigation, Software, Visualization. **Wenhui Ge:** Investigation, Data curation. **Junhui Liu:** Data curation, Resources. **Yi Yu:** Supervision, Conceptualization. **Xiaoyan Xie:** Conceptualization, Methodology, Validation.

Declaration of competing interest

The authors declare that they have no known competing financial interests or personal relationships that could have appeared to influence the work reported in this paper.

Data availability

Data will be made available on request.

Appendix A. Supplementary data

Supplementary data to this article can be found online at https://doi.org/10.1016/j.mtbio.2023.100782.

References

[1] C. Warinner, J.F.M. Rodrigues, R. Vyas, C. Trachsel, N. Shved, J. Grossmann, A. Radini, Y. Hancock, R.Y. Tito, S. Fiddyment, Pathogens and host immunity in the ancient human oral cavity, Nat. Genet. 46 (2014) 336–344.

[2] P. Toche, L. Salinas, M.M. Guzmán, S. Afani, A. Jadue, Recurrent oral ulcer: clinical characteristic and differential diagnosis, Rev. Chil. infectol.: Organo Oficial de la Sociedad Chilena de Infectologia. 24 (2007) 215–219.
[3] B. Yalçın, H.Y. Seçkin, G. Kalkan, Z. Takci, Y. Önder, R. Çitil, S. Demir, Ş. Şahin, Investigation of Behçet's disease and recurrent aphthous stomatitis frequency: the highest prevalence in Turkey, Balkan Med. J. 33 (2016) 390–395.
[4] P. Thakrar, S.I. Chaudhry, Oral ulceration: an overview of diagnosis and management, Prim. Dent. J. 5 (2016) 30–33.
[5] Y. Zhou, M. Wang, C. Yan, H. Liu, D.-G. Yu, Advances in the application of electrospun drug-loaded nanofibers in the treatment of oral ulcers, Biomolecules 12 (2022) 1254.
[6] E.L. Vieira, A.J. Leonel, A.P. Sad, N.R. Beltrão, T.F. Costa, T.M. Ferreira, A. C. Gomes-Santos, A.M. Faria, M.C. Peluzio, D.C. Cara, Oral administration of sodium butyrate attenuates inflammation and mucosal lesion in experimental acute ulcerative colitis, J. Nutr. Biochem. 23 (2012) 430–436.
[7] J.E. Raber-Durlacher, I. Von Bültzingslöwen, R.M. Logan, J. Bowen, A.R. Al-Azri, H. Everaus, E. Gerber, J.G. Gomez, B.G. Pettersson, Y. Soga, Systematic review of cytokines and growth factors for the management of oral mucositis in cancer patients, Support. Care Cancer 21 (2013) 343–355.
[8] Y. Sudhakar, K. Kuotsu, A. Bandyopadhyay, Buccal bioadhesive drug delivery—a promising option for orally less efficient drugs, J. Contr. Release 114 (2006) 15–40.
[9] K. Hijazi, T. Lowe, C. Meharg, S.H. Berry, J. Foley, G.L. Hold, Mucosal microbiome in patients with recurrent aphthous stomatitis, J. Dent. Res. 94 (2015) 87s–94s.
[10] R.-Q. Wu, D.-F. Zhang, E. Tu, Q.-M. Chen, W. Chen, The mucosal immune system in the oral cavity—an orchestra of T cell diversity, Int. J. Oral Sci. 6 (2014) 125–132.
[11] G. Guan, Q. Zhang, Z. Jiang, J. Liu, J. Wan, P. Jin, Q. Lv, Multifunctional silk fibroin methacryloyl microneedle for diabetic wound healing, Small 18 (2022), 2203064.
[12] S.D.C. Santos, N.C. Fávaro-Moreira, H.B. Abdalla, G.G.X. Augusto, Y.M. Costa, M. C. Volpato, F.C. Groppo, H.S. Gill, M. Franz-Montan, A crossover clinical study to evaluate pain intensity from microneedle insertion in different parts of the oral cavity, Int. J. Pharm. (Amst.) 592 (2021), 120050.
[13] M.I. Nasiri, L.K. Vora, J.A. Ershaid, K. Peng, I.A. Tekko, R.F. Donnelly, Nanoemulsion-based dissolving microneedle arrays for enhanced intradermal and transdermal delivery, Drug Deliv. Trans. Re. 12 (2022) 881–896.
[14] H. He, X. Zhang, L. Du, M. Ye, Y. Lu, J. Xue, J. Wu, X. Shuai, Molecular Imaging Nanoprobes for Theranostic Applications, Adv Drug Deliver Rev, 2022, 114320.
[15] C. Liu, Z. Zhou, G. Liu, Q. Wang, J. Chen, L. Wang, Y. Zhou, G. Dong, X. Xu, Y. Wang, Efficacy and safety of dexamethasone ointment on recurrent aphthous ulceration, Am. J. Med. 125 (2012) 292–301.
[16] C. Zhang, Y. Liu, W. Li, P. Gao, D. Xiang, X. Ren, D. Liu, Mucoadhesive buccal film containing ornidazole and dexamethasone for oral ulcers: in vitro and in vivo studies, Pharmaceut. Dev. Technol. 24 (2019) 118–126.
[17] X. Zhang, X. Kang, L. Jin, J. Bai, W. Liu, Z. Wang, Stimulation of wound healing using bioinspired hydrogels with basic fibroblast growth factor (bFGF), Int. J. Nanomed. 13 (2018) 3897.
[18] F. Kobayashi, K. Matsuzaka, T. Inoue, The effect of basic fibroblast growth factor on regeneration in a surgical wound model of rat submandibular glands, Int. J. Oral Sci. 8 (2016) 16–23.
[19] L. Lei, X. Wang, Y. Zhu, W. Su, Q. Lv, D. Li, Antimicrobial hydrogel microspheres for protein capture and wound healing, Mater. Des. 215 (2022), 110478.
[20] M. Su, L. Ruan, X. Dong, S. Tian, W. Lang, M. Wu, Y. Chen, Q. Lv, L. Lei, Current state of knowledge on intelligent-response biological and other macromolecular hydrogels in biomedical engineering: a review, Int. J. Biol. Macromol. 227 (2023) 472–492.
[21] Z. Xu, G. Liu, P. Liu, Y. Hu, Y. Chen, Y. Fang, G. Sun, H. Huang, J. Wu, Hyaluronic acid-based glucose-responsive antioxidant hydrogel platform for enhanced diabetic wound repair, Acta Biomater. 147 (2022) 147–157.
[22] Y. Yuan, T. Nie, Y. Fang, X. You, H. Huang, J. Wu, Stimuli-responsive cyclodextrin-based supramolecular assemblies as drug carriers, J. Mater. Chem. B 10 (2022) 2077–2096.
[23] V.S. Meka, M.K. Sing, M.R. Pichika, S.R. Nali, V.R. Kolapalli, P. Kesharwani, A comprehensive review on polyelectrolyte complexes, Drug Discov. Today 22 (2017) 1697–1706.
[24] M. Rahimi, R. Ahmadi, H.S. Kafil, V. Shafiei-Irannejad, A novel bioactive quaternized chitosan and its silver-containing nanocomposites as a potent antimicrobial wound dressing: structural and biological properties, Mater. Sci. Eng., C 101 (2019) 360–369.
[25] J. Xie, Y. Ji, W. Xue, D. Ma, Y. Hu, Hyaluronic acid-containing ethosomes as a potential carrier for transdermal drug delivery, Colloids Surf. B Biointerfaces 172 (2018) 323–329.
[26] W.C. Ngeow, C.C. Tan, Y.C. Goh, T.M. Deliberador, C.W. Cheah, A narrative review on means to promote oxygenation and angiogenesis in oral wound healing, Bioengineering 9 (2022) 636.
[27] A.Z. Abo-shady, H. Elkammar, V.S. Elwazzan, M. Nasr, Formulation and clinical evaluation of mucoadhesive buccal films containing hyaluronic acid for treatment of aphthous ulcer, J. Drug Deliv. Sci. Technol. 55 (2020), 101442.
[28] H.-Y. Park, D.-K. Kweon, J.-K. Kim, Molecular weight-dependent hyaluronic acid permeability and tight junction modulation in human buccal TR146 cell monolayers, Int. J. Biol. Macromol. 227 (2023) 182–192.
[29] P. Makvandi, M. Kirkby, A.R.J. Hutton, M. Shabani, C.K.Y. Yiu, Z. Baghbantaraghdari, R. Jamaledin, M. Carlotti, B. Mazzolai, V. Mattoli, R. F. Donnelly, Engineering microneedle patches for improved penetration: analysis, skin models and factors affecting needle insertion, Nano-Micro Lett. 13 (2021) 93.
[30] V.C. Shunmugasamy, M. AbdelGawad, M.U. Sohail, T. Ibrahim, T. Khan, T.D. Seers, B. Mansoor, In vitro and in vivo study on fine-grained Mg-Zn-RE-Zr alloy as a biodegradable orthopedic implant produced by friction stir processing, Bioact. Mater. 28 (2023) 448–466.
[31] R. Zare, H. Abdolsamadi, S. Soleimani Asl, S. Radi, H. Bahrami, S. Jamshidi, The bFGF can improve angiogenesis in oral mucosa and accelerate wound healing, Rep Biochem Mol Biol 11 (2023) 547–552.
[32] A. El-Howati, M.H. Thornhill, H.E. Colley, C. Murdoch, Immune mechanisms in oral lichen planus, Oral Dis. 29 (2023) 1400–1415.
[33] D. Campoccia, L. Montanaro, C.R. Arciola, A review of the biomaterials technologies for infection-resistant surfaces, Biomaterials 34 (2013) 8533–8554.
[34] J. Cui, X. Ji, Y. Mi, Q. Miao, F. Dong, W. Tan, Z. Guo, Antimicrobial and antioxidant activities of N-2-Hydroxypropyltrimethyl ammonium chitosan derivatives bearing amino acid Schiff bases, Mar. Drugs 20 (2022) 86.
[35] Z. Yang, Q. Cui, R. An, J. Wang, X. Song, Y. Shen, M. Wang, H. Xu, Comparison of microbiomes in ulcerative and normal mucosa of recurrent aphthous stomatitis (RAS)-affected patients, BMC Oral Health 20 (2020) 128.
[36] H. Yuan, J. Qiu, T. Zhang, X. Wu, J. Zhou, S. Park, Quantitative changes of Veillonella, Streptococcus, and Neisseria in the oral cavity of patients with recurrent aphthous stomatitis: a systematic review and meta-analysis, Arch. Oral Biol. 129 (2021), 105198.
[37] D. Zhu, T.K. Johnson, Y. Wang, M. Thomas, K. Huynh, Q. Yang, V.C. Bond, Y. E. Chen, D. Liu, Macrophage M2 polarization induced by exosomes from adipose-derived stem cells contributes to the exosomal proangiogenic effect on mouse ischemic hindlimb, Stem Cell Res. Ther. 11 (2020) 1–14.
[38] L. Alarcon-Martinez, S. Yilmaz-Ozcan, M. Yemisci, J. Schallek, K. Kılıç, A. Can, A. Di Polo, T. Dalkara, Capillary pericytes express α-smooth muscle actin, which requires prevention of filamentous-actin depolymerization for detection, Elife 7 (2018), e34861.
[39] D. Wen, T. Liang, G. Chen, H. Li, Z. Wang, J. Wang, R. Fu, X. Han, T. Ci, Y. Zhang, Adipocytes encapsulating telratolimod recruit and polarize tumor-associated macrophages for cancer immunotherapy, Adv. Sci. 10 (5) (2023), 2206001.
[40] M. Weber, H. Steinle, S. Golombek, L. Hann, C. Schlensak, H.P. Wendel, M. Avci-Adali, Blood-contacting biomaterials: in vitro evaluation of the hemocompatibility, Front. Bioeng. Biotechnol. 6 (2018) 99.